Trans. Japan Soc. Aero. Space Sci.
Vol. 46, No. 152, pp. 61–67, 2003

Coupled Librational and Orbital Motions of a Large-Scale Spacecraft*

By Noboru TAKEICHI,[1] M. C. NATORI,[2] Nobukatsu OKUIZUMI[2] and Ken HIGUCHI[2]

[1] *Department of Aeronautics and Astronautics, Graduate School of Engineering, The University of Tokyo, Tokyo, Japan*
[2] *The Institute of Space and Astronautical Science, Sagamihara, Japan*

(Received June 7th, 2002)

Mechanical characteristics of coupled librational and orbital motions of a large-scale spacecraft are investigated. A rigid body of an arbitrary shape is considered as a mathematical model, and a set of nonlinear equations of motion about the librational and orbital motions is formulated. Through Lindstedt's perturbation method, approximated analytical solutions are obtained. From the analytical solutions, the conditions of instability are clarified, and the characteristics of the orbital motion are shown. The total mechanical energy has the minimum value when the librational and orbital motions coincide with the periodic solution. The formula for the total mechanical energy proves that the periodic solution is the minimum energy solution. From the nonlinear numerical investigations, it is shown that the results stated above are valid even without any approximations. The results of this study provide us the fundamental understandings of the dynamics of large-scale spacecraft in space.

Key Words: Large-Scale Spacecraft, Attitude Motion, Orbital Motion, Coupling

Nomenclature

a :	semimajor axis
d :	dimension factor of spacecraft, Eq. (17)
e :	orbital eccentricity
I :	moment of inertia of spacecraft
k :	shape factor of spacecraft, Eq. (18)
M :	mass of spacecraft
n_0 :	orbital mean motion
r :	orbital radius
r_{peri} :	orbital radius at perigee
$x_{\mathrm{I}}, y_{\mathrm{I}}, z_{\mathrm{I}}$:	inertial coordinate
$x_{\mathrm{o}}, y_{\mathrm{o}}, z_{\mathrm{o}}$:	orbital coordinate
$x_{\mathrm{B}}, y_{\mathrm{B}}, z_{\mathrm{B}}$:	body fixed coordinate
μ :	Earth gravitational constant
ν :	true anomaly
ψ :	pitch angle
Subscripts	
c :	coupled
d :	decoupled
i :	initial conditions
p :	periodic solutions

1. Introduction

The dimensions of large-scale spacecraft, such as solar-power satellites, tethered systems, etc., are not small enough to be negligible compared to the dimensions of their orbits. In such situations, the effects of coupling between librational and orbital motions are not negligible. In previous studies including coupling, orbital motions are mainly focused,[1–4] and the orbit controls through the attitude motions of spacecraft are also investigated.[5–8] In these studies, however, the stability of librational motion is not considered.

The orbits of actual spacecraft cannot coincide exactly with complete circular orbits, even if their reference orbits are circular. A tethered system is intentionally planned to have an elliptic orbit of a large eccentricity.[9] The attitude motion is always subjected to disturbances from the orbital motion, and the control actuators are limited in terms of capacity and methods, especially in the case of flexible large-scale spacecraft. Therefore, sometimes the attitude motion cannot be controlled to stay along the gravity-gradient direction, and some motion is inevitable. In previous papers, periodic solutions are focused,[3, 10–12] and the stability of attitude motion is investigated through stability analysis of the periodic solution. Active controls toward the periodic solution are also studied.[13] However, mechanical characteristics of the periodic solution have not been clarified.

In this study, we focus on the stability of the free librational motion and the characteristics of coupled motion over a long period of operation. The equations of motion including coupling become highly nonlinear. Therefore, at first, approximated analytical solutions are found through Lindstedt's perturbation method.[14] From the analytical solutions, the stability and mechanical characteristics of motion are investigated. Next, the results obtained from the analytical solutions are examined using nonlinear numerical methods. Since coupling is considered, we can treat the whole system as a conservative one, and it is possible to focus on the total mechanical energy. In the investigations, the orbital eccentricity is simultaneously considered to clarify the mechanical meanings of the periodic solution in elliptic orbits.

*Presented at 23rd International Symposium on Space Technology and Science, Matsue, Japan, May 30, 2002

2. Formulation

2.1. System configurations and assumptions

A spacecraft in an orbit is approximated as a rigid body. The model and coordinates are shown in Fig. 1. Only in-plane motion is focused, and only gravitational force is considered. Active control of the librational and orbital motions is not considered.

2.2. Equations of motion

Equations of motion are obtained using the Lagrange formulation. The position vector $\boldsymbol{x}_\mathrm{I}$ of a small particle with its mass of dm in the inertial coordinate is given as follows:

$$\boldsymbol{x}_\mathrm{I} = r\begin{pmatrix}\cos\nu\\ \sin\nu\end{pmatrix} + x_\mathrm{B}\begin{pmatrix}\sin(\nu+\psi)\\ -\cos(\nu+\psi)\end{pmatrix} + y_\mathrm{B}\begin{pmatrix}\cos(\nu+\psi)\\ \sin(\nu+\psi)\end{pmatrix} \tag{1}$$

The kinetic energy K is given as follows:

$$\begin{aligned} K &= \int \frac{1}{2}\|\dot{\boldsymbol{x}}_\mathrm{I}\|^2 \mathrm{d}m \\ &= \int \left(\frac{1}{2}(x_\mathrm{B}^2 + y_\mathrm{B}^2)(\dot{\nu}+\dot{\psi})^2 + \frac{1}{2}(r^2\dot{\nu}^2 + \dot{r}^2)\right)\mathrm{d}m \\ &= \frac{1}{2}I_z(\dot{\nu}+\dot{\psi})^2 + \frac{1}{2}M(r^2\dot{\nu}^2+\dot{r}^2) \end{aligned} \tag{2}$$

where,

$$\begin{cases} I_x = \int (y_\mathrm{B}^2 + z_\mathrm{B}^2)\mathrm{d}m \\ I_y = \int (z_\mathrm{B}^2 + x_\mathrm{B}^2)\mathrm{d}m \\ I_z = \int (x_\mathrm{B}^2 + y_\mathrm{B}^2)\mathrm{d}m \end{cases} \tag{3}$$

The potential energy U is given as follows:

$$\begin{aligned} U &= -\int \frac{\mu}{\|\boldsymbol{x}_\mathrm{I}\|}\mathrm{d}m \\ &= -\int \frac{\mu}{\sqrt{x_\mathrm{B}^2 + y_\mathrm{B}^2 + r^2 + 2r(x_\mathrm{B}\sin\psi + y_\mathrm{B}\cos\psi)}}\mathrm{d}m \\ &\cong -\int \left(\frac{\mu}{r} + \frac{\mu(x_\mathrm{B}^2 + y_\mathrm{B}^2 - 3(x_\mathrm{B}^2 - y_\mathrm{B}^2)\cos 2\psi)}{4r^3}\right)\mathrm{d}m \\ &= -\frac{\mu M}{r} - \frac{\mu(I_z + 3(I_x - I_y)\cos 2\psi)}{4r^3} \end{aligned} \tag{4}$$

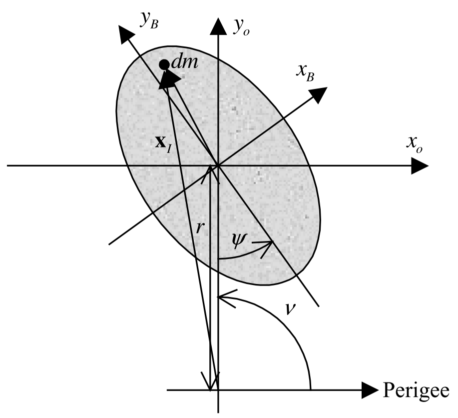

Fig. 1. The coordinates of the system.

The Lagrangian L is obtained as

$$L = K - U \tag{5}$$

and the Lagrange equation of motion is obtained:

$$\frac{\mathrm{d}}{\mathrm{d}t}\left(\frac{\partial L}{\partial \dot{q}}\right) - \frac{\partial L}{\partial q} = 0 \tag{6}$$

Finally, the equations of the librational motion of the spacecraft ψ, the orbital angular velocity $\dot{\nu}$, and the orbital radius r are obtained as follows:

$$\ddot{\psi} = -\ddot{\nu} - \frac{3\mu}{r^3}\frac{I_x - I_y}{I_z}\sin\psi\cos\psi \tag{7}$$

$$\ddot{\nu} = -\frac{2Mr\dot{r}\dot{\nu} + I_z\ddot{\psi}}{I_z + Mr^2} \tag{8}$$

$$\ddot{r} = -\frac{\mu}{r^2} + r\dot{\nu}^2 - \frac{3\mu(I_z + 3(I_x - I_y)\cos 2\psi)}{4Mr^4} \tag{9}$$

3. Analytical Investigation

3.1. Approximated analytical solutions

In this section, a set of approximated analytical solutions is obtained through Lindstedt's perturbation method. The orbital eccentricity e and the dimension factor d (Eq. (17)) are considered as small parameters of first and second order, respectively. In the following formulation, e and d are substituted by a small parameter ε, and terms over second order are neglected.

$$\begin{cases} e = O(\varepsilon) \\ d = O(\varepsilon^2) \end{cases} \tag{10}$$

The decoupled orbit is approximated as a function of time as follows:[15)]

$$\dot{\nu}_\mathrm{d} = n_0\left(1 + 2e\cos n_0 t + \frac{5}{2}e^2\cos 2n_0 t\right) \tag{11}$$

$$r_\mathrm{d} = a\left(1 + \frac{1}{2}e^2 - e\cos n_0 t - \frac{1}{2}e^2\cos 2n_0 t\right) \tag{12}$$

where, n_0 and a satisfy the following equation:

$$\mu = n_0^2 a^3 \tag{13}$$

The approximated analytical solutions are assumed as follows:

$$\psi = \psi_0 + \varepsilon\cdot\psi_1 + \varepsilon^2\cdot\psi_2 \tag{14}$$

$$\dot{\nu}_\mathrm{c} = \dot{\nu}_\mathrm{d} + \varepsilon^2\dot{\nu}_2 \tag{15}$$

$$r_\mathrm{c} = r_\mathrm{d} + \varepsilon^2 r_2 \tag{16}$$

We define d and k as follows:

$$d = \frac{I_z}{Ma^2} \tag{17}$$

$$k^2 = 3\frac{I_x - I_y}{I_z} \quad (0 \le k^2 \le 3) \tag{18}$$

The following approximations are made.

$$\begin{cases} \sin\psi\cos\psi \approx \psi \\ \cos 2\psi \approx 1 - 2\psi^2 \end{cases} \tag{19}$$

A new independent variable $\tau = nt$ is introduced, where n is defined as follows:

$$n = n_0 + \varepsilon \cdot n_1 + \varepsilon^2 \cdot n_2 \tag{20}$$

By the definitions and assumptions cited above, the following set of equations is obtained through the approximations. (In the equations, the prime denotes the differentiation by τ.)

$$\psi_0'' + k^2\psi_0 = 0 \tag{21}$$

$$\psi_1'' + k^2\psi_1 = -3ek^2\cos n_0 t \cdot \psi_0 - \frac{2n_1}{n_0}\psi_0'' + 2e\sin n_0 t \tag{22}$$

$$\ddot{\nu}_2 = -\frac{2n_0}{a}\dot{r}_2 - d\ddot{\psi}_0 \tag{23}$$

$$\ddot{r}_2 = -\frac{3}{4}adn_0^2(1 + k^2 - 2k^2\psi_0^2) + 3n_0^2 r_2 + 2an_0\dot{\nu}_2 \tag{24}$$

$$\begin{aligned}\psi_2'' + k^2\psi_2 = &-\left(\frac{n_1^2}{n_0^2} + 2\frac{n_2}{n_0}\right)\psi_0'' - 3ek^2\cos n_0 t \cdot \psi_1 - \frac{2n_1}{n_0}\psi_1'' \\ &+ 5e^2\sin 2n_0 t - \frac{1}{n_0^2}\ddot{\nu}_2 + \left(-\frac{3}{2}e^2 - \frac{9}{2}e^2\cos 2n_0 t + \frac{3}{a}r_2\right)k^2\psi_0\end{aligned} \tag{25}$$

These equations provide the solutions recursively as follows:

$$\psi_0 = A\cos(knt + \theta_1) \tag{26}$$

$$\psi_1 = \frac{2e}{k^2 - 1}\sin(n_0 t) + \frac{3k^2 e}{-4k + 2}A\cos(-n_0 t + knt + \theta_1) + \frac{3k^2 e}{4k + 2}A\cos(n_0 t + knt + \theta_1) \tag{27}$$

$$\begin{aligned}\dot{\nu}_2 = n_0\bigg(&\frac{3}{8}d(1 + (1 - A^2)k^2) + 3B_1 + 2B_2\cos(n_0 t + \theta_2) \\ &+ \frac{dk(k^2+3)}{k^2 - 1}A\sin(knt + \theta_1) + \frac{3dk^2}{2(4k^2 - 1)}A^2\cos(2knt + 2\theta_1)\bigg)\end{aligned} \tag{28}$$

$$r_2 = a\left(-2B_1 - B_2\cos(n_0 t + \theta_2) - \frac{2dk}{k^2 - 1}A\sin(knt + \theta_1) - \frac{3dk^2}{4(4k^2 - 1)}A^2\cos(2knt + 2\theta_1)\right) \tag{29}$$

$$\begin{aligned}\psi_2 = &\frac{9e^2k^2(k-1)}{32k - 16}A\cos(2n_0 t - knt - \theta_1) + \frac{9e^2k^2(k+1)}{32k + 16}A\cos(2n_0 t + knt + \theta_1) \\ &+ \frac{e^2(2k^2 - 5)}{(k^2 - 4)(k^2 - 1)}\sin(2n_0 t) + \frac{3dk^3}{(4k^2 - 1)(k^2 - 1)}A^2\sin(2knt + 2\theta_1) \\ &+ \frac{9dk^2}{64(4k^2 - 1)}A^3\cos(3knt + 3\theta_1) + \frac{2B_2}{k^2 - 1}\sin(n_0 t + \theta_2) \\ &- \frac{3B_2k^2}{4k - 2}A\cos(knt - n_0 t + \theta_1 - \theta_2) + \frac{3B_2k^2}{4k + 2}A\cos(knt + n_0 t + \theta_1 + \theta_2)\end{aligned} \tag{30}$$

$$n_1 = 0 \tag{31}$$

$$n_2 = n_0\left(\frac{k^2 + 3}{2(k^2 - 1)}d + \frac{9k^2}{16(4k^2 - 1)}A^2 d + \frac{3(k^2 - 1)}{4(4k^2 - 1)}e^2 + 3B_1\right) \tag{32}$$

A and θ_1 are the initial conditions determined by librational motion, and B_1, B_2 and θ_2 are those determined by orbital motion, where $B_i = O(\varepsilon^2)$. The analytical solution is obtained by substituting Eqs. (26)–(32) into Eqs. (14)–(16) and (20). To focus on the effects of the coupling, B_i is determined so that the coupled orbit has the same average orbital energy and orbital angular momentum as a Keplerian orbit. As a result, we obtain $B_1 = 3/8(1 + (1 - A^2)k^2)d$ and B_2 as an arbitrary value. B_2 is denoted as B in the following. We can assume $\theta_2 = 0$, because θ_2 affects only the initial argument of perigee. Finally, we obtain the following set of approximated analytical solutions (33)–(36).

$$\psi = A\cos(knt+\theta) + \frac{2(e+B)}{k^2-1}\sin(n_0t) + \frac{e^2(2k^2-5)}{(k^2-4)(k^2-1)}\sin(2n_0t)$$
$$+ \frac{3k^2(e+B)}{-4k+2}A\cos(-n_0t+knt+\theta) + \frac{3k^2(e+B)}{4k+2}A\cos(n_0t+knt+\theta)$$
$$+ \frac{9e^2k^2(k-1)}{-16+32k}A\cos(2n_0t-knt-\theta) + \frac{9e^2k^2(k+1)}{16+32k}A\cos(2n_0t+knt+\theta)$$
$$+ \frac{3dk^3}{(4k^2-1)(k^2-1)}A^2\sin(2knt+2\theta) + \frac{9dk^2}{64(4k^2-1)}A^3\cos(3knt+3\theta) \tag{33}$$

$$\dot{\nu}_{\mathrm{c}} = \dot{\nu}_{\mathrm{d}} + n_0\left(\frac{3}{2}d(1+(1-A^2)k^2) + 2B\cos(n_0t)\right.$$
$$\left. + \frac{dk(k^2+3)}{k^2-1}A\sin(knt+\theta) + \frac{3dk^2}{2(4k^2-1)}A^2\cos(2knt+2\theta)\right) \tag{34}$$

$$r_{\mathrm{c}} = r_{\mathrm{d}} + a\left(-\frac{3}{4}d(1+(1-A^2)k^2) - B\cos(n_0t)\right.$$
$$\left. - \frac{2dk}{k^2-1}A\sin(knt+\theta) - \frac{3dk^2}{4(4k^2-1)}A^2\cos(2knt+2\theta)\right) \tag{35}$$

where,

$$n = n_0\left(1 + \frac{9k^4+4k^2+3}{8(k^2-1)}d - \frac{9k^2(8k^2-3)}{16(4k^2-1)}A^2d + \frac{3(k^2-1)}{4(4k^2-1)}e^2\right) \tag{36}$$

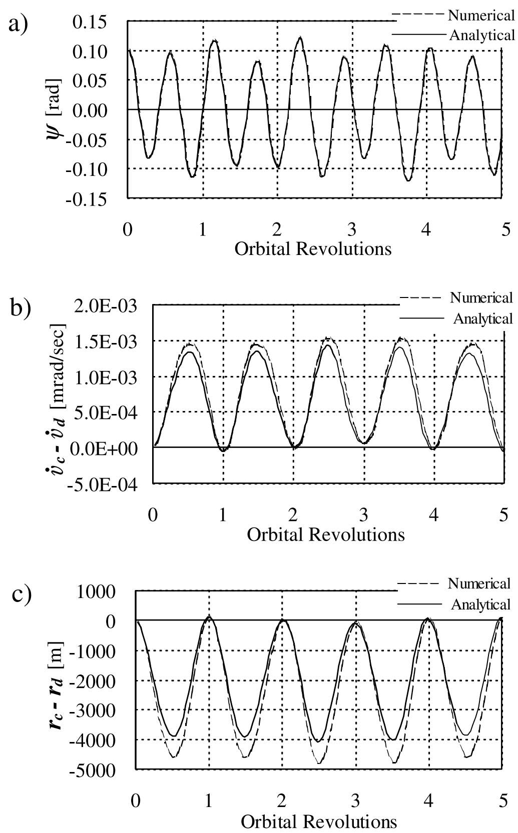

Fig. 2. Analytical and numerical solutions: a) pitch motion, b) orbital angular velocity, c) orbital radius.

When the coupling effects are not included, that is, $d = 0$ and $B = 0$, solutions (33) and (36) coincide exactly with Beletskii's solution.[3)] To evaluate the validity of analytical solutions (33)–(36), a nonlinear numerical solution of the equations of motion (7)–(9) is also obtained for $r_{\mathrm{peri}} = 6678$ [km], $e = 0.02$, $d = 1.0 \times 10^{-4}$, and $k^2 = 3$. Figure 2 shows the comparison between the analytical and numerical solutions. Figure 2a shows librational motion, and Figs. 2b and c show the difference of the orbital motion from the Keplerian orbit. In all figures, good correspondence is found, which shows the validity of the analytical solutions. From the process mentioned above, analytical solutions have been obtained for a spacecraft of an arbitrary shape and arbitrary dimension in an orbit of arbitrary eccentricity, as far as the approximation is valid.

3.2. Discussions of analytical solution set

In Eqs. (33)–(35), the terms concerning d become unstable only when $k^2 = 1$ and $k^2 = 1/4$. These conditions are the same as those when the terms concerning e become unstable.[3)] The orbital angular velocity is faster than that of the Keplerian orbit, and the difference is $3/2 \cdot d(1+(1-A^2)k^2)n_0$ on average. The orbital radius is smaller, and the difference is $3/4 \cdot d(1+(1-A^2)k^2)a$. The shift of the orbital angular velocity results in the secular movement of the argument of perigee.

Because the effects of coupling are included, the whole system is conservative. The total mechanical energy E_{T} is obtained as a constant value as follows:

$$E_{\mathrm{T}} = K + U$$
$$= -\frac{1}{2}Ma^2n_0^2 - \frac{1}{4}d(k^2-1)Ma^2n_0^2 + \frac{1}{2}dA^2k^2Ma^2n_0^2 \tag{37}$$

From Eq. (37), we can find that the total mechanical energy has the minimum value when $A = 0$. When $A = 0$, any perturbation on the attitude motion always leads the system to have larger total mechanical energy. We obtain the following solution set for $A = 0$:

$$\psi = \frac{2(e+B)}{k^2-1}\sin(n_0 t) + \frac{e^2(2k^2-5)}{(k^2-4)(k^2-1)}\sin(2n_0 t) \tag{38}$$

$$\dot{\nu}_c = \dot{\nu}_d + n_0\left(2B\cos n_0 t + \frac{3}{2}d(1+k^2)\right) \tag{39}$$

$$r_c = r_d + a\left(-B\cos n_0 t - \frac{3}{4}d(1+k^2)\right) \tag{40}$$

In the solutions, only the constant and oscillation terms appear, which have the same period as the orbital period. Therefore, the solution set when $A = 0$ is a periodic solution with one orbital period. It is concluded that the total mechanical energy has the minimum value when the motion of the system coincides with the periodic solution.

4. Nonlinear Numerical Investigation

4.1. Stability of motion

In this section, nonlinear numerical investigations are carried out to evaluate the validity of the results obtained by the analytical investigations. Especially, we focus on situations where the approximations of d and e (Eq. (10)) are invalid and the nonlinearity must be included.

In previous papers, which do not include the coupling effects, it is known that librational motion is stable if a stable periodic solution exists.[3,10,11] It may be reasonable to consider that, even if the coupling effects are included, the stability of the motion is investigated through analyzing the existence of the stable periodic solution. In this study, the shooting method[16] is applied to investigate the periodic solution and its stability. In the numerical analyses, the following parameters are used:

$$r_{peri} = 6678\,[\text{km}], \quad e = 0.2, \quad M = 1000\,[\text{kg}] \tag{41}$$

$$I_x = I_z = 6.97 \times 10^{11\text{–}14}\,[\text{kg}\cdot\text{m}^2], \quad I_y = 0\,[\text{kg}\cdot\text{m}^2] \tag{42}$$

and the initial orbital parameters are given the same as that of the Keplerian orbit at the perigee as follows:

$$r_i = r_{peri}, \quad \dot{r}_i = 0, \quad \nu_i = 0, \quad \dot{\nu}_i = \sqrt{\frac{(1+e)\mu}{r_i^3}} \tag{43}$$

The values of I_x, I_y, and I_z give $k^2 = 3$, and $d = 1.0 \times 10^{-5}$–1.0×10^{-2}, and they correspond to a tethered system with a length of 52.8–1670 [km], which consists of two identical masses. In the analyses, the periodic solutions, which have the same period as that of the Keplerian orbit, are numerically obtained. The results show that stable periodic solutions are obtained in all cases. This means that the effects of coupling do not affect stability even without any approximations. Figure 3 shows the motion of the periodic solution when $d = 3.58 \times 10^{-5}$, which corresponds to a tethered system with a length of 100 [km]. Figures 3b and c show the difference between the coupled orbital motion and Keplerian orbit.

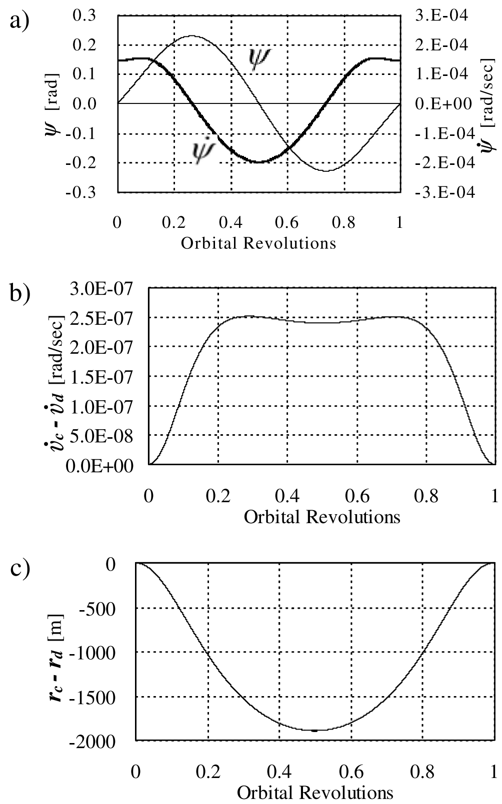

Fig. 3. Periodic solution: a) pitch motion, b) orbital angular velocity, c) orbital radius.

4.2. Dynamic behavior

To investigate the dynamic behavior, numerical simulations for 500 orbital revolutions are carried out using the values shown in Eq. (41), $d = 3.58 \times 10^{-5}$ and $k^2 = 3$. The initial librational motion is given as $\psi_i = 0$ and $\dot{\psi}_i = 0$, which does not coincide with that of the periodic solution, and initial orbital conditions are given the same as Eq. (43). Figure 4a is the time-history of ψ during the initial 100 revolutions. Figure 4b shows Poincaré maps of ψ–$\dot{\psi}$ and r–$\dot{\nu}$ during 500 revolutions. In this study, Poincaré maps are made by sampling the values of states when the orbital radius becomes locally minimum at every revolution. The time interval is not constant because the orbit does not coincide with the Keplerian orbit. In the Poincaré maps, all points are on closed curves, which means the motion is quasi-periodic and stable. The change of the orbit is shown in Fig. 5. In the figure, only the beginning and 500th orbits are depicted. The orbit continues to have the same semimajor axis and eccentricity on average, and the argument of perigee moves secularly 1.47 [mrad] per one revolution, which takes about 376 days to revolve once around the earth.

4.3. Mechanical meanings of periodic solution

To investigate the meanings of the periodic solution, several numerical simulations have been carried out using $d = 3.58 \times 10^{-5}$ and $k^2 = 3$. In the simulations, several values of the initial pitch rate $\dot{\psi}_0$ are given, and the initial orbital parameters are determined so that the total mechanical energy

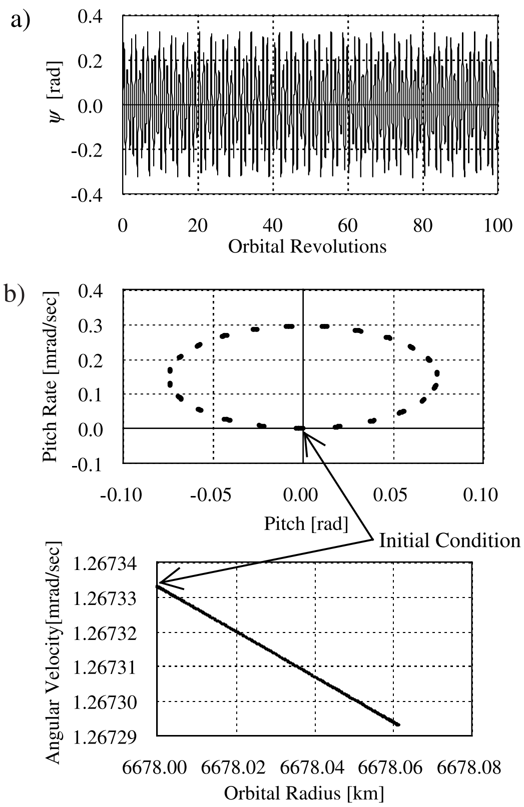

Fig. 4. Dynamic behavior: a) pitch motion, b) Poincaré maps.

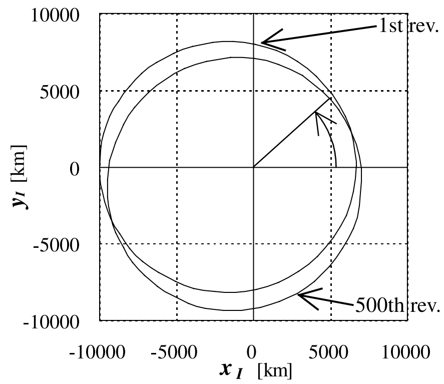

Fig. 5. Movement of argument of perigee.

E_T and total angular momentum M_T have the same values as when $\dot{\psi}_i = 0$, $r_{peri} = 6678$ [km], and $e = 0.2$ at the perigee, where M_T is defined as follows:

$$M_T = Mr^2\dot{\nu} + I_z(\dot{\psi} + \dot{\nu}) \tag{44}$$

The mechanical energy about the attitude motion of the spacecraft E_a is defined as follows:

$$E_a = \frac{1}{2}I_z(\dot{\nu} + \dot{\psi})^2 - \frac{\mu(I_z + 3(I_x - I_y)\cos 2\psi)}{4r^3} \tag{45}$$

Although an exchange between the orbital energy and attitude motion energy always occurs, it is not accumulative. Therefore, it is meaningful to check the average attitude motion energy $\bar{E}_a$, which is calculated as follows:

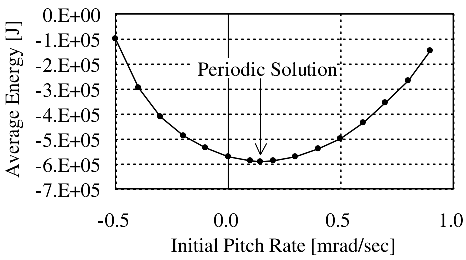

Fig. 6. Average attitude motion energy.

$$\bar{E}_a = \lim_{T\to\infty} \frac{1}{T}\int_0^T E_a \mathrm{d}t \tag{46}$$

The values of $\bar{E}_a$ for 500 revolutions are calculated and shown in Fig. 6. When the initial condition coincides with the periodic solution, the mean attitude motion energy $\bar{E}_a$ has the minimum value. In other cases, the amplitude of the attitude motion is larger. This result agrees with that obtained from the analytical solution set.

5. Conclusion

The coupled librational and orbital motions of a large-scale spacecraft are investigated.

From the analytical solution set obtained through the perturbation method, the qualitative characteristics have been clarified. The analytical solution set shows that the motion is stable except for a few values in the moment of inertia ratios. The solution set also provides the equations of the effects of coupling on orbital motion. The total mechanical energy is formulated, and it is shown that total mechanical energy has the minimum value when the motion coincides with the periodic solution. This means that the periodic solution is the minimum energy solution, and some perturbation of librational motion always leads the total mechanical energy to have a larger value. If the orbital parameters are fixed, librational motion has the minimum energy when it coincides with the periodic solution.

The nonlinear equations of motion are also investigated numerically. From analyzing the periodic solutions and their stability, it is shown that coupling does not affect stability over a wide range of spacecraft dimensions. The Poincaré maps also show stable coupled motion. From the several numerical simulations, the mean attitude motion energy becomes minimum when motion coincides with the periodic solution. We can consider that the results obtained from the analytical solutions are still valid even without any approximations.

References

1) Moran, J. M.: Effects of Plane Librations on the Orbital Motion of a Dumbbell Satellite, *ARS J.*, **31** (1961), pp. 1089–1096.
2) Yu, E. Y.: Long-Term Coupling Effects between Librational and Orbital Motions of a Satellite, *AIAA J.*, **2** (1964), pp. 553–555.
3) Beletskii, V. V.: Motion of an Artificial Satellite about Its Center of Mass, NASA TT F-429, 1966.

4) Cho, S., Lovell, T. A., Cochran, J. E., Jr. and Cicci, D. A.: Approximate Solutions for Tethered Satellite Motion, *AIAA J. Guidance*, **24** (2001), pp. 746–754.
5) Murakami, C.: On Orbit Control Using Gravity Gradient Effects, *Acta Astronautica*, **8** (1981), pp. 733–747.
6) Martines-Sanchez, M. and Gavit, S. A.: Orbital Modification Using Forced Tether-Length Variations, *AIAA J. Guidance*, **10** (1987), pp. 233–241.
7) Landis, G. A.: Reactionless Orbital Propulsion Using Tether Deployment, *Acta Astronautica*, **26** (1992), pp. 307–312.
8) Watanabe, Y. and Nakamura, Y.: Orbit Control for a Spacecraft via the Gravity Gradient Force, IAF Paper 98-A.2.08, 49th International Astronautical Congress, Melbourne, Australia, 1998.
9) Oyama, K., Sasaki, S., Su, Y. and Balan, N.: Feasibility Study of a Tethered Satellite System, Proc. of the 18th International Symposium on Space Technology and Science (ISTS), Kagoshima, Japan, May 17–22, 1992, pp. 1851–1858.
10) Modi, V. J. and Brereton, R. C.: Periodic Solutions Associated with the Gravity-Gradient-Oriented System: Part I. Analytical and Numerical Determination, *AIAA J.*, **7** (1969), pp. 1217–1225.
11) Modi, V. J. and Brereton, R. C.: Periodic Solutions Associated with the Gravity-Gradient-Oriented System: Part II. Stability Analysis, *AIAA J.*, **7** (1969), pp. 1465–1468.
12) Takeichi, N., Natori, M. C. and Okuizumi, N.: In-Plane/Out-of-Plane Librations of a Tethered System in Elliptical Orbits, *Trans. Jpn. Soc. Aeronaut. Space Sci.*, **43** (2001), pp. 196–202.
13) Takeichi, N., Natori, M. C. and Okuizumi, N.: Fundamental Strategies for Deployment and Libration Control of a Tethered System in Elliptical Orbits, IAF Paper 01-A.4.08, 52nd International Astronautical Congress, Toulouse, France, 2001.
14) Meirovitch, L.: Elements of Vibration Analysis, McGraw-Hill, New York, 1975, pp. 364–368.
15) Battin, R. H.: An Introduction to the Mathematics and Methods of Astrodynamics, AIAA Education Series, AIAA, Inc., Washington, DC, 1987, pp. 199–205.
16) Parker, T. S. and Chua, L. O.: Practical Numerical Algorithms for Chaotic Systems, Springer-Verlag, New York, 1989.